The use of polynomial chaos for parameter identification from measurements in nonlinear dynamical systems

ARTICLE *in* ZAMM JOURNAL OF APPLIED MATHEMATICS AND MECHANICS: ZEITSCHRIFT FÜR ANGEWANDTE MATHEMATIK UND MECHANIK · JANUARY 2014

Impact Factor: 1.16 · DOI: 10.1002/zamm.201300232

1 AUTHOR:

Sayan Gupta
Indian Institute of Technology Madras
48 PUBLICATIONS **254** CITATIONS

The Use of Polynomial Chaos for Parameter Identification from Measurements in Nonlinear Dynamical Systems

Rangaraj P, Abhijit Chaudhuri, and Sayan Gupta *

Department of Applied Mechanics, Indian Institute of Technology Madras, Chennai 600036, India

Received XXXX, revised XXXX, accepted XXXX
Published online XXXX

Key words particle filter, Polynomial chaos, System identification, Duffing oscillator, oscillating airfoil, fluid structure interaction

This study focuses on the development of a computationally efficient algorithm for the offline identification of system parameters in nonlinear dynamical systems from noisy response measurements. The proposed methodology is built on the bootstrap particle filter available in the literature for dynamic state estimation. The model and the measurement equations are formulated in terms of the system parameters to be identified - treated as random variables, with all other parameters being considered as internal variables. Subsequently, the problem is transformed into a mathematical subspace spanned by a set of orthogonal basis functions obtained from polynomial chaos expansions of the unknown system parameters. The bootstrap filtering carried out in the transformed space enables identification of system parameters in a computationally efficient manner. The efficiency of the proposed algorithm is demonstrated through two numerical examples - a Duffing oscillator and a fluid structure interaction problem involving an oscillating airfoil in an unsteady flow.

1 Introduction

Predicting the system response by solving the associated equations of motion, with appropriate initial and boundary conditions, essentially involves the solution of the forward problem and leads to the time history of the system response. In contrast, identification of the system parameters from the available time history measurements of the system response, is an inverse problem. The solution of inverse problems is a much more computationally challenging exercise than solving the forward problem. The difficulties associated with the identification of the system parameters from measurement data can be attributed to the noise that invariably exist in all measurements, erroneous calibration of the measurement sensors, incomplete measurement data, imprecise model for the system arising due to insufficient knowledge and lack of understanding about the physics associated with the system and incomplete knowledge about the parameters associated with the system. These difficulties imply that inverse problems are ill-posed, often leading to situations with non-unique solutions or solutions that are physically unfeasible.

A mathematically rigorous approach to the solution of inverse problems has been to employ the principles of Bayesian theories to estimate the unknown parameters in a system. The underlying principle of such frameworks is based on treating the model parameters to be identified as random variables or random fields, with assumed probability density functions. For a dynamical system expressed in the following general first order differential form

$$\dot{\mathbf{X}}(t) = \mathbf{f}(\mathbf{X}(t), \boldsymbol{\theta}(t), t), \tag{1}$$

$\boldsymbol{\theta}(t)$ represents the vector of system parameters to be identified. Here, $\mathbf{X}(t)$ is the measurable metric of the dynamical system, usually defined in terms of the state vector, the vector function $\mathbf{f}(\,\cdot\,)$ represents typically a nonlinear function available either explicitly or in implicit form and t is time. The probability density function (pdf) for $\boldsymbol{\theta}(t)$ at time instant t, is denoted by $p_{\boldsymbol{\theta}}(\boldsymbol{\theta}; t)$. Here, $p_{\boldsymbol{\theta}}(\boldsymbol{\theta}; t = t_0) \equiv p_{\boldsymbol{\theta}}(\boldsymbol{\theta})$ is referred to as the prior density function and takes into account information available about $\boldsymbol{\theta}$ at initial time $t = t_0$. If no information is available, a model for $p_{\boldsymbol{\theta}}(\boldsymbol{\theta})$ is assumed such that its support is defined within a practically feasible domain. The solution of the forward problem enables probabilistic characterization of the observable metric $\mathbf{X}$ at time t. Subsequently, using available measurement data $\mathbf{D}$, the posterior pdf for $\boldsymbol{\theta}$ can be expressed in terms of Baye's theorem as

$$p(\boldsymbol{\theta}|\mathbf{D}) = \frac{p(\mathbf{D}|\boldsymbol{\theta}) p_{\boldsymbol{\theta}}(\boldsymbol{\theta})}{\int p(\mathbf{D}|\boldsymbol{\theta}) p_{\boldsymbol{\theta}}(\boldsymbol{\theta})\, \mathrm{d}\boldsymbol{\theta}}. \tag{2}$$

* Corresponding author: E-mail: gupta.sayan@gmail.com, Phone: +91 44 2257 4055, Fax: +91 44 2257 4052

Here, the conditional pdf $p(\mathbf{D}|\boldsymbol{\theta})$ is the normalized likelihood function. This procedure of updating the pdf of the system parameters can be carried out recursively for each time step for which measurements are available, with the *posteriori* pdf at time step t_k taken to be the prior density for time step t_{k+1}. This procedure of Bayesian updating ensures that the associated variability in the pdf decrease as more measurements are assimilated leading to fairly accurate estimates of the system parameters with quantifiable confidence bounds.

The development of the equations for estimating the *posteriori* pdf from available measurements and extracting relevant information from it constitute the essence of dynamic state estimation techniques. Typically, this involves the evaluation of multi-dimensional integrals whose dimensions equal the size of the vector $\boldsymbol{\theta}$. Closed form analytical solutions for these integrals are possible only for a special class of problems leading to the Kalman filter [1]. Methods which are variants of the Kalman filter, have been developed for parameter identification in problems in a more general setting [2–11]. However, these methods are usually iterative in nature, lacks universality in application and can be computationally expensive without a commensurate increase in robustness or accuracy. Alternative methods that rely on obtaining asymptotic approximations for the evaluation of these multi-dimensional integrals [12] or using numerical quadrature rules [13] have also been discussed.

However, the advent of cheap computing facilities have ensured the use of Monte Carlo simulations to approximate multi-dimensional integrals as a viable alternative [14]. This has led to the development of Monte Carlo based Bayesian algorithms [15–25], commonly known as particle filters, for parameter identification from measurements. The primary advantages of particle filters lie in their general nature and wide applicability for problems even with high degrees of nonlinearity. These methods have been used for system identification in a wide variety of problems such as, climate modeling [26], geophysics [27, 28], heat transfer [29, 30] and structural health monitoring [31–37]. Particle filters require the solution of the forward problem for a large number of realizations for $\boldsymbol{\theta}$, generated using Monte Carlo simulations and evaluating their likelihood when compared with the measurement data. This needs to be carried out for all the available measurements. The drawback of the particle filtering approaches lie in the computational costs involved in solving the forward problem a large number of times, corresponding to each measurement data set. This becomes computationally infeasible for complex problems where a solution of a single forward problem require significant computational costs.

The focus of this paper is on developing a methodology for reducing computational costs associated with particle filters. The central challenge lies in accelerating the solution of the forward problem for the set of sample realizations of $\boldsymbol{\theta}$. This can be achieved by developing surrogate models for the system such that the solution of the forward problem is simple. Response surface based methods [38, 39] are simple to implement but lack mathematical rigor and are not universally applicable. An alternative approach built on more rigorous mathematical foundations would be to use stochastic spectral methods to represent the structure response as a function of the unknown system parameters. This study adopts the latter approach. Here, the underlying principle lies in projecting the forward problem into a space spanned by orthogonal stochastic functions and carrying out the filtering in this space. The basis stochastic functions are usually polynomial functions of random variables and are collectively referred to as polynomial chaos (PC) [40]. Typically, the random basis functions constitute Hermite polynomials of standard Gaussian random variables $\boldsymbol{\xi}$. The proposed method in this paper essentially transforms the Bayesian problem of parameter identification from the space spanned by $\boldsymbol{\theta}$ to a mathematical subspace spanned by the random basis functions. This is achieved by projecting the forward problem into the random subspace and expressing the measurable metric in terms of the polynomial chaos functions. The filtering is subsequently carried out in the transformed subspace $\boldsymbol{\xi}$.

This paper is organized as follows: First, the problem of parameter identification of dynamical systems is formulated mathematically. The mathematical equations underlying the development of the basic equations under Bayesian settings are presented. A variant of the particle filters - the bootstrap particle filter - is discussed in details, highlighting the difficulties associated with this approach. The following section reviews the concept of Wiener chaos expansion and discussions are presented on how the PC can be used to accelerate the identification algorithm. The section on numerical examples presents two examples to highlight the proposed method. The salient features of this study are summarized in the concluding section.

2 The Particle Filter

The differential equation for the nonlinear dynamical system in Eq. (1) can be recast into the recursive form as

$$\mathbf{X}_{k+1} = \tilde{\mathbf{f}}_k(\mathbf{X}_k, \boldsymbol{\theta}_k), \tag{3}$$

where, $\mathbf{X}_k \in \Re^n$ is a n-dimensional vector that denotes the state of the dynamical system, at time step $t = t_k$, $\tilde{\mathbf{f}}_k(\,\cdot\,)$ is the functional form that relates $\mathbf{X}_{k+1}$ to $\mathbf{X}_k$ and the suffix k represents the time step $t = t_k$. In modeling the physical system using Eq. (1) or Eq. (3), unknown errors are introduced into the model due to simplifying assumptions and unmodelled phenomena arising due to incomplete understanding or ignorance. These errors are incorporated into the model by assuming

them to be modeled as a random process. Thus, Eq. (3) can be recast as

$$\mathbf{X}_{k+1} = \tilde{\mathbf{g}}_k(\mathbf{X}_k, \boldsymbol{\theta}_k, \mathbf{w}_k). \tag{4}$$

Here, $\mathbf{w}_k \in \Re^m$ is the discretized m-dimensional vector of the discretized noise process consisting of a vector of correlated random variables and $\tilde{\mathbf{g}}_k(\,\cdot\,)$ is typically a nonlinear function, such that, $\tilde{\mathbf{g}}_k(\,\cdot\,) : \Re^n \times \Re^m \rightarrow \Re^n$.

Usually, $\mathbf{X}_k$ is not directly measurable. Instead, sensors measure parameters, $\mathbf{Z}_k$, that are calibrated to map the measurements to $\mathbf{X}_k$. Thus, a relationship can be defined between the actual parameters measured and $\mathbf{X}_k$ through the measurement equation

$$\mathbf{Z}_k = \tilde{\mathbf{h}}_k(\mathbf{X}_k, \mathbf{v}_k; \boldsymbol{\theta}_k). \tag{5}$$

Here, $\mathbf{Z}_k \in \Re^p$ is a p-dimensional vector of measurements at time t_k, $\mathbf{v}_k \in \Re^r$ is a r-dimensional vector of a sequence of random variables which collectively represents the noise in the measurements and calibration errors, and $\tilde{\mathbf{h}}_k(\,\cdot\,) : \Re^n \times \Re^r \rightarrow \Re^p$ is a typically nonlinear function that relates the measurements $\mathbf{Z}_k$ to $\mathbf{X}_k$. The model and the measurement equations given by Eqs. (4-5) are standard forms that are available in the dynamic state estimation literature where the focus is on estimating $\mathbf{X}_k$. However, in system identification the focus is on estimating $\boldsymbol{\theta}$. Introducing the augmented vector $\mathbf{Y}_k = [\mathbf{X}_k, \boldsymbol{\theta}_k]$ and rewriting the model and the measurement equations in terms of $\mathbf{Y}_k$, the identification algorithms can be used to estimate $\mathbf{Y}_k$. However, such an approach increases the dimension of the identification problem. Alternatively, the model and measurement equations, given by Eqs. (4-5), can be rewritten only in terms of $\boldsymbol{\theta}_k$ with $\mathbf{X}_k$ being considered as internal variables. This leads to rewriting the model equation (also called the process equation) as

$$\boldsymbol{\theta}_{k+1} = \mathbf{g}_k(\boldsymbol{\theta}_k, \mathbf{w}_k) \tag{6}$$

and the measurement equation as

$$\mathbf{Z}_k = \mathbf{h}_k(\boldsymbol{\theta}_k, \mathbf{v}_k). \tag{7}$$

Note that the functions $\mathbf{g}_k(\cdot)$ and $\mathbf{h}_k(\cdot)$ are distinct from $\tilde{\mathbf{g}}_k(\cdot)$ and $\tilde{\mathbf{h}}_k(\cdot)$ used earlier. Rewriting the model and the measurement equations only in terms of $\boldsymbol{\theta}_k$ - the parameters to be identified with $\mathbf{X}_k$ being treated as internal variables, ensures a dimensional reduction in the system identification problem leading to enhancement of computational efficiency [35].

Since both $\boldsymbol{\theta}_k$ and $\mathbf{Z}_k$ are corrupted by unknown errors $\mathbf{w}_k$ and $\mathbf{v}_k$, complete characterization of $\boldsymbol{\theta}_k$ is possible only in terms of $p(\boldsymbol{\theta}_k|\mathbf{D}_k)$, the posterior density function of $\boldsymbol{\theta}_k$ when conditioned on the available measurements $\mathbf{D}_k = \{\mathbf{Z}_1, \mathbf{Z}_2, \ldots, \mathbf{Z}_k\}$. Assuming that the prior density at time $t = t_0$ to be given by

$$p(\boldsymbol{\theta}_1|\mathbf{D}_0) \equiv p(\boldsymbol{\theta}_0), \tag{8}$$

a prediction for the pdf for $\boldsymbol{\theta}_k$, conditioned on past measurements $\mathbf{D}_{k-1}$ can be expressed in terms of a recursive equation of the form

$$p(\boldsymbol{\theta}_k|\mathbf{D}_{k-1}) = \int p(\boldsymbol{\theta}_k|\boldsymbol{\theta}_{k-1}) p(\boldsymbol{\theta}_{k-1}|\mathbf{D}_{k-1})\ \mathrm{d}\boldsymbol{\theta}_{k-1}. \tag{9}$$

Here, $p(\boldsymbol{\theta}_k|\boldsymbol{\theta}_{k-1})$ is the pdf of the evolution of $\boldsymbol{\theta}$ at different time instants and is expressed as

$$p(\boldsymbol{\theta}_k|\boldsymbol{\theta}_{k-1}) = \int p(\boldsymbol{\theta}_k|\boldsymbol{\theta}_{k-1}, \mathbf{w}_{k-1}) p(\mathbf{w}_{k-1})\ \mathrm{d}\mathbf{w}_k. \tag{10}$$

In writing Eq. (10) it is assumed that $\mathbf{w}_k$ is independent of $\boldsymbol{\theta}_k$ and thus $p(\mathbf{w}_{k-1}|\boldsymbol{\theta}_{k-1}) \equiv p(\mathbf{w}_{k-1})$. From the model equation in Eq. (6), it can be shown that

$$p(\boldsymbol{\theta}_k|\boldsymbol{\theta}_{k-1}, \mathbf{w}_{k-1}) \equiv \delta(\boldsymbol{\theta}_k - \mathbf{g}_{k-1}(\boldsymbol{\theta}_{k-1}, \mathbf{w}_{k-1})), \tag{11}$$

where, $\delta(\,\cdot\,)$ is the Dirac-delta equation. Substituting Eqs. (10-11) in Eq. (9) leads to

$$p(\boldsymbol{\theta}_k|\mathbf{D}_{k-1}) = \int\int \delta(\boldsymbol{\theta}_k - \mathbf{g}_{k-1}(\boldsymbol{\theta}_{k-1}, \mathbf{w}_{k-1})) p(\mathbf{w}_{k-1}) p(\boldsymbol{\theta}_{k-1}|\mathbf{D}_{k-1})\ \mathrm{d}\mathbf{w}_k\ \mathrm{d}\boldsymbol{\theta}_{k-1}. \tag{12}$$

Equation (12) is the recursive form of the prediction equation. Once the measurements $\mathbf{Z}_k$ are available at time step k, the prediction can be updated using the Bayesian relation

$$p(\boldsymbol{\theta}_k|\mathbf{D}_k) = \frac{p(\mathbf{Z}_k|\boldsymbol{\theta}_k) p(\boldsymbol{\theta}_k|\mathbf{D}_{k-1})}{p(\mathbf{Z}_k|\mathbf{D}_{k-1})}, \tag{13}$$

where the normalizing denominator is

$$p(\mathbf{Z}_k|\mathbf{D}_{k-1}) = \int p(\mathbf{Z}_k|\boldsymbol{\theta}_k)p(\boldsymbol{\theta}_k|\mathbf{D}_{k-1})\ \mathrm{d}\boldsymbol{\theta}_k. \tag{14}$$

Here, $p(\boldsymbol{\theta}_k|\mathbf{D}_{k-1})$ is available from Eq. (9) and $p(\mathbf{Z}_k|\boldsymbol{\theta}_k)$ can be obtained from Eq. (7) as

$$\begin{aligned} p(\mathbf{Z}_k|\boldsymbol{\theta}_k) &= \int p(\mathbf{Z}_k|\boldsymbol{\theta}_k, \mathbf{v}_k)p(\mathbf{v}_k)\ \mathrm{d}\mathbf{v}_k \\ &= \int \delta(\mathbf{Z}_k - \mathbf{h}_k(\boldsymbol{\theta}_k, \mathbf{v}_k))p(\mathbf{v}_k)\ \mathrm{d}\mathbf{v}_k. \end{aligned} \tag{15}$$

In Eq. (15), $p(\mathbf{Z}_k|\boldsymbol{\theta}_k, \mathbf{v}_k)$ is represented as the Dirac-delta function as $\mathbf{Z}_k$ is known deterministically if $\boldsymbol{\theta}_k$ and $\mathbf{v}_k$ are known. In writing the above equation, the underlying assumption is that the measurement noise $\mathbf{v}_k$ is independent of $\boldsymbol{\theta}_k$. Equations (6-15) constitute the formal solution for the Bayesian identification algorithm in the reduced $\boldsymbol{\theta}_k$-space.

2.1 The Bootstrap Particle Filter

Since the functions $\mathbf{g}_k(\,\cdot\,)$ and $\mathbf{h}_k(\,\cdot\,)$ are typically nonlinear, closed form solutions for the multi-dimensional integrals in Eqs. (6-15) are not possible and one has to resort to approximate methods for evaluating them. Quadrature schemes for the numerical evaluation of these integrals are not efficient when the dimension of these integrals is large. Monte Carlo simulations could be used for approximating these multi-dimensional integrals. However, this requires simulating a large number of sample realizations for $\boldsymbol{\theta}$ at every time step where the Bayesian updating is carried out and solving the forward problem. This forms the essence of particle filters. A set of samples for $\boldsymbol{\theta}$ are simulated according to the prior density function and the forward problem is solved deterministically for each realization. Subsequently, once the measurements become available, the pdf for $\boldsymbol{\theta}$ are updated following Eqs. (6-15). This predictor-corrector approach is carried out efficiently in a recursive format using the bootstrap particle filter algorithm [15]. The key steps in the implementation of the bootstrap filtering algorithm is summarized as follows:

1. Consider the k-th time step $t = t_k$. Assume $p(\boldsymbol{\theta}_{k-1} \mid \mathbf{D}_{k-1})$ is known. For $k = 0$, this is the prior density function $p(\boldsymbol{\theta}_{k-1} \mid \mathbf{D}_{k-1}) \equiv p(\boldsymbol{\theta}_0)$. Simulate N samples of the vector of random samples $\{\boldsymbol{\theta}_{k-1}\}_{i=1}^N$. Similarly, assume a prior density function for $p(\mathbf{w}_{k-1})$ and generate samples for $\{\mathbf{w}_{k-1}\}_{i=1}^N$.
2. Each sample is passed through the system model in Eq. (6) to obtain the predictions for the state at time step k. Thus,
$$\boldsymbol{\theta}_k^{*(i)} = \mathbf{g}_{k-1}(\boldsymbol{\theta}_{k-1}^{(i)}, \mathbf{w}_{k-1}^{(i)}). \tag{16}$$
3. Once the measurements $\mathbf{Z}_k$ is available, the likelihood corresponding to each prediction $\{\boldsymbol{\theta}_k^{*(i)}\}_{i=1}^N$ is evaluated as $\mathcal{L}(\mathbf{Z}_k|\boldsymbol{\theta}_{k_j}^*) = \mathbf{Z}_k - \mathbf{h}_k(\boldsymbol{\theta}_k^*)$.
4. An approximation for $p(\mathbf{Z}_k|\boldsymbol{\theta}_{k_j}^*)$ is obtained by normalizing the likelihood function as
$$q_j = \frac{\mathcal{L}(\mathbf{Z}_k \mid \boldsymbol{\theta}_k^{*(j)})}{\sum_{j=1}^N \mathcal{L}(\mathbf{Z}_k \mid \boldsymbol{\theta}_k^{*(j)})}, \tag{17}$$
where $\mathcal{L}(\,\cdot\,)$ is the likelihood function.
5. The discrete probability mass function for the next iterate is defined as
$$P[\boldsymbol{\theta}_{k_j} = \boldsymbol{\theta}_k^*] = q_j. \tag{18}$$
6. From the discrete probability mass function in Eq. (18), a new set of N samples for $\boldsymbol{\theta}_k$ are generated.
7. The mean of the estimates are obtained by averaging across the ensemble, and is expressed as
$$\bar{\boldsymbol{\theta}}_{k|k} = \frac{1}{N}\sum_{j=1}^N \boldsymbol{\theta}_{k_j}. \tag{19}$$
The corresponding standard deviation of the estimate is calculated as
$$\boldsymbol{\sigma}_{k|k} = \sqrt{\frac{1}{N-1}\sum_{j=1}^N (\boldsymbol{\theta}_{k_j} - \bar{\boldsymbol{\theta}}_{k|k})^T(\boldsymbol{\theta}_{k_j} - \bar{\boldsymbol{\theta}}_{k|k})}. \tag{20}$$

8. The above steps are repeated by setting $k = k + 1$. In this way, the filtering is carried out for the entire available time history of measurements.

The application of the bootstrap filtering algorithm (BFA) requires N evaluations of the forward problem, defined by Eq. (6) corresponding to each measurement data. For M measurement data points, the application of BFA requires $M \times N$ evaluations of Eq. (6). This can prove to be a major drawback of the approach, especially if each evaluation of Eq. (6) involves significant computational time. This is especially true for highly nonlinear dynamical systems. The crux of making the method computationally less expensive lies in reducing the computational effort required in solving the forward problem in Eq. (6). This study focuses on increasing the computational efficiency of BFA by adopting a polynomial chaos based approach for solving the forward problem. A brief review of the relevant concepts related to polynomial chaos expansions is presented in the next section, followed by discussions on how this method can be used in conjunction with BFA to make the parameter identification problem computationally efficient.

3 The Polynomial Chaos Expansion

The method of polynomial chaos expansion involves projecting a random variable or a random field in an orthogonal basis subspace spanned by a set of orthogonal polynomials of random variables. This method has its origins in the works of [40] and can be extremely useful for the solution of stochastic differential equations. In its original form, the expansion employed Hermite polynomials from the Askey scheme, whose support consisted of a vector of standard Gaussian random variables. Subsequently, the expansion was formalized through the Cameron-Martin theorem leading to the representation of a second order stationary random process $\theta(t)$ as

$$\theta(t) = a_0(t)\Psi_o + \sum_{i_1=1}^{\infty} a_{i_1}(t)\Psi_1(\xi_{i_1}) + \sum_{i_1=1}^{\infty}\sum_{i_1=1}^{\infty} a_{i_1 i_2}\Psi_2(\xi_{i_1}, \xi_{i_2}) + \ldots, \tag{21}$$

where, $\Psi_n(\xi_{i_1}, \xi_{i_2}, \ldots, \xi_{i_n})$ is the Hermite polynomial of order n in terms of n-dimensional vector $\boldsymbol{\xi} = \{\xi_{i_1}, \ldots, \xi_{i_n}\}$ of standard Gaussian random variables. Equation (21) can be compactly written as

$$\theta(t, \boldsymbol{\xi}) = \sum_{j=0}^{\infty} a_j(t)\Psi_j(\boldsymbol{\xi}), \tag{22}$$

where, $\{\Psi_j(\boldsymbol{\xi})\}$ constitute a set of orthogonal Hermite polynomials of $\boldsymbol{\xi}$, $a_j(t) = \mathrm{E}[\theta(t, \boldsymbol{\xi})\Psi_j(\boldsymbol{\xi})]$ are the deterministic projections of the random process and $\mathrm{E}[\cdot]$ is the expectation operator. The first few 1-D Hermite polynomials are given by

$$\Psi_0(\xi) = 1, \quad \Psi_1(\xi) = \xi, \quad \Psi_2(\xi) = (\xi^2 - 1), \ldots \tag{23}$$

and the higher order Hermite polynomials can be generated from the recursive equation

$$\Psi_n(\xi) = \xi\Psi_{n-1}(\xi) - (n-1)\Psi_{n-2}(\xi). \tag{24}$$

For 2-D Hermite polynomials, the first few polynomials according to the Askey scheme are as follows

$$\begin{aligned} &\Psi_0(\xi_1, \xi_2) = 1, \ \ \Psi_1(\xi_1, \xi_2) = \xi_1, \ \ \Psi_2(\xi_1, \xi_2) = \xi_2, \\ &\Psi_3(\xi_1, \xi_2) = \xi_1^2 - 1, \ \ \Psi_4(\xi_1, \xi_2) = \xi_1\xi_2, \ \ \Psi_5(\xi_1, \xi_2) = \xi_2^2 - 1, \ldots \end{aligned} \tag{25}$$

An approximation for the series expansion in Eq. (22) can be obtained by truncating the series to P terms, where

$$P = \frac{(n + n_p)!}{n!n_p!} - 1, \tag{26}$$

when n is the dimension of $\boldsymbol{\xi}$ and n_p is the highest order of the Hermite polynomials. The corresponding truncated series is referred to as p-order PCE expansion. The condition that $\theta(t, \boldsymbol{\xi})$ is a second order stationary process implies that $\mathrm{E}[\theta(t, \boldsymbol{\xi})^2] < \infty$ which in turn, means that the truncated polynomial series converges in L^2 to $\theta(t, \boldsymbol{\xi})$.

The spectral representation of a random variable $\theta \equiv \theta(\boldsymbol{\xi})$ can also be obtained using Eq. (22) where the projections $a_j(t) \equiv a_j$ are no longer functions of t. The spectral representation for a random variable is possible if $\mathrm{E}[\theta(\boldsymbol{\xi})^2] < \infty$. This condition, however, places no constraint on the continuity of the function $\theta(\boldsymbol{\xi})$. The polynomial chaos expansion can be generalized to the space spanned by other orthogonal polynomials from the generalized Askey scheme where the support constitutes standard non-Gaussian random variables [41].

3.1 Response Analysis using PCE

Polynomial chaos expansions are an useful tool for solving differential equations having random non-homogeneous terms or when the coefficients of the differential equations constitute random fields or random variables. For a simple nonlinear oscillator with an unknown time varying parameter $\theta(t)$, Eq. (1) can be simplified to

$$\dot{U}(t) = g(U(t), \theta(t), t) \tag{27}$$

where, $g(\,\cdot\,)$ is an operator and $U(t)$ is the response. A polynomial chaos approach to response characterization requires decomposing the uncertain input $\theta(t)$ along the stochastic dimensions as in Eq. (22), truncated to P terms. This implies that the response $U(t)$ is also random whose spectral representation is also of the same form as in Eq. (22) but whose projections along the stochastic dimensions are unknowns. This section reviews the methods for characterization of $U(t)$ using PCE. The methods discussed in the literature can be classified as intrusive and non-intrusive. Brief descriptions of these approaches are presented next.

3.2 Galerkin Polynomial Chaos Approach

In Galerkin PC approach, the chaos expansion of the system response is substituted into the governing equations leading to a set of coupled equations in terms of the chaos coefficients [42]. These coupled deterministic equations typically have terms, such as, $\mathrm{E}[\Psi_i(\boldsymbol{\xi})\Psi_j(\boldsymbol{\xi})\ldots\Psi_k(\boldsymbol{\xi})]$ as coefficients. For nonlinear dynamical systems, the form of these coupled deterministic equations are usually complicated and their solution can be tedious and time consuming. Depending on the nonlinearity, the number of terms in these expectations could be large. Evaluation of these terms imply multidimensional integration and need to be carried out prior to the solution of the coupled deterministic equations. As the original differential equations get substantially modified in terms of the chaos coefficients, the Galerkin's approach to solving the stochastic differential equations using PCE is termed as an intrusive approach.

3.3 Non-intrusive Projection Method

The underlying principle of nonintrusive methods is to arrive at an approximation for the projections along the different random dimensions directly by solving the forward problem deterministically corresponding to the collocation points in the probability space. Thus, the projections can be directly evaluated as

$$a_j(t) = \frac{\mathrm{E}[U(t,\boldsymbol{\xi})\Phi_j(\boldsymbol{\xi})]}{\mathrm{E}[\Phi_j^2(\boldsymbol{\xi})]}. \tag{28}$$

Note that $\mathrm{E}[\Phi_j(\boldsymbol{\xi})\Phi_k(\boldsymbol{\xi})] = 0$ for $j \neq k$. When $\boldsymbol{\xi}$ are standard normal, assuming $\Phi(\boldsymbol{\xi})$ to be Hermite polynomials leads to an exponential convergence of the series representation. The collocation points can be chosen as the zeros of the Hermite polynomials and a Gauss-Hermite quadrature scheme can be used for evaluating the expectations in Eq. (28). This implies that the problem defined in Eq. (27) need to be solved deterministically corresponding to the collocation points defined in the probability space. For a differential equation with multiple random coefficients, the collocation grids need to be constructed using tensor products of the one dimensional grids. This is true even if the differential equation is a function of a random field as the random field can be assumed to be discretized into a collection of correlated random variables.

4 Particle Filtering and Polynomial Chaos

The principle ideas of polynomial chaos expansion and bootstrap particle filtering can now be integrated to develop a particle filtering methodology which is computationally cheaper and more efficient. This involves decomposing the system parameters $\boldsymbol{\theta}_k$ as a polynomial chaos expansion, given by

$$\theta_{k_i}(\boldsymbol{\xi}) = \sum_{j=0}^{P} a_j \Psi_j(\boldsymbol{\xi}), \tag{29}$$

where, θ_{k_i} is the i-th component of $\boldsymbol{\theta}_k$, $\{\Psi_j\}_{j=0}^{\infty}$ constitute a set of orthogonal polynomials from the Askey scheme and are functions of random variables $\boldsymbol{\xi}$, a_j are the corresponding projections along the bases and the series is truncated to P terms determined from Eq. (26). Note that the dimension of $\boldsymbol{\xi}$ is greater than or equal to the dimension of $\boldsymbol{\theta}_k$.

The forward problem, defined by Eq. (6), can also be spectrally decomposed along the same basis functions. This leads to representing the i^{th} component of $\boldsymbol{\theta}_{k+1}$ as

$$\theta_{k+1_i}(\boldsymbol{\xi}) = \sum_{j=0}^{P} b_j \Psi_j(\boldsymbol{\xi}), \tag{30}$$

where, the projections b_j on the random basis functions can be evaluated from Eq. (28). Here, $U(t, \boldsymbol{\xi})$ in Eq. (28) should be replaced by $\theta_{k+1_i}(\boldsymbol{\xi})$ as it is the solution of the forward problem defined in Eq. (6). Now the particle filter algorithm can be applied using two different approaches.

4.1 Approach 1

The first approach involves the following steps:

1. For $k = 0$, assuming that the pdf $p(\boldsymbol{\theta}_0)$ is known, a polynomial chaos expansion for $\boldsymbol{\theta}_k$ is obtained from Eq. (29).
2. For $k = 1$, the prior predictions $\boldsymbol{\theta}_k^*$ need to be calculated from the forward model represented by Eq. (6). This is achieved using PCE by representing $\boldsymbol{\theta}_{k+1}$ as the series in Eq. (30), whose projections b_j are evaluated from Eq. (28).
3. The remaining steps are identical to the steps in section 2.1.

The idea in this approach is that once the prior pdf of the parameters are known at a particular time step, the appropriate orthogonal set of polynomials are chosen from the Askey scheme as well as the corresponding pdf $p(\boldsymbol{\xi})$ for the support $\boldsymbol{\xi}$. An approximation for the solution of the forward problem is obtained as a polynomial chaos expansion whose coefficients are determined from Eq. (28). This step requires the solution of the forward problem equal to the number of collocation points. Drawing samples of $\{\boldsymbol{\xi}_i\}_{i=1}^N$ from $p(\boldsymbol{\xi})$ leads to realizations of $\{\boldsymbol{\theta}_{k_i}\}_{i=1}^N$. The corresponding forward problem is computed in an inexpensive manner by substituting $\{\boldsymbol{\xi}_i\}_{i=1}^N$ in Eq. (30).

As the pdf of $\boldsymbol{\theta}$ is obtained numerically at different time steps while the particle filter algorithm is applied, the chances are high that the prior density at a particular time step will not be a standard pdf. In such situations, one can use the arbitrary polynomial chaos expansions as the basis functions [43, 44]. This would ensure a faster convergence of the series expansion.

4.2 Approach 2

The approach described in the previous section requires estimating the random projections b_j at each time instant where the filtering is carried out. It is obvious that this approach would be computationally cheaper as long as $N > n$, where n is the number of collocation points required for estimating the coefficients b_j in Eq. (28). On the other hand, significant savings in computational effort could be effected if the need for fitting a PCE at each step could be avoided. Noting that Eqs. (29-30) can be expressed as a function of the same set of random variables $\boldsymbol{\xi}$, Eq. (6) can be recast in terms of $\boldsymbol{\xi}$ as the primary variables. This leads to the following form for the model equation

$$\boldsymbol{\xi}_{k+1} = \mathbf{g}_k(\sum_{j=0}^{P} a_j \Psi_j(\boldsymbol{\xi}_k), \mathbf{w}_k) = \hat{\mathbf{g}}_k(\boldsymbol{\xi}_k, \mathbf{w}_k), \tag{31}$$

and the corresponding measurement equation as

$$\mathbf{Z}_k = \mathbf{h}_k(\sum_{j=0}^{P} a_j \Psi_j(\boldsymbol{\xi}_k), \mathbf{v}_k) = \hat{\mathbf{h}}_k(\boldsymbol{\xi}_k, \mathbf{v}_k). \tag{32}$$

Note that $\hat{\mathbf{g}}_k(\cdot)$ and $\hat{\mathbf{h}}_k(\cdot)$ are different from $\tilde{\mathbf{g}}_k(\cdot)$ and $\tilde{\mathbf{h}}_k(\cdot)$ used earlier. Here, $\boldsymbol{\theta}_k$ are now treated as internal variables and do not appear explicitly in the equations. By expressing the model and the measurement equations as in Eqs. (31-32), the parameter identification problem is now transformed from the $\boldsymbol{\theta}_k$-space to $\boldsymbol{\xi}_k$-space. However, the development of the equations for the dynamic state estimation does not get affected in any other way and the filtering is now carried out in the $\boldsymbol{\xi}_k$-space.

Despite transforming the problem to the $\boldsymbol{\xi}_k$-space, computational efficiency will not be achieved unless the solution of the forward problem in Eq. (31) can be bypassed. This is achieved by decomposing $\boldsymbol{\xi}_{k+1}$ as a PCE and representing as

$$\boldsymbol{\xi}_{k+1} = \sum_{i=0}^{P} b_i \Psi_i(\boldsymbol{\xi}_k). \tag{33}$$

Here, the coefficients b_i are estimated using Eq. (28) only at the start of the filtering and need not be repeated at each time step. This is a very crucial step in the proposed formulation as once the coefficients in Eq. (33) are available, the solution of the forward problem is easily obtained by substituting for $\boldsymbol{\xi}_k$ without the need for the evaluation of the actual function $\mathbf{g}_k(\cdot)$. The key steps in this approach are summarized as follows:

1. Assume that the pdf $p(\boldsymbol{\theta}_0)$ is known for $k = 0$. Also, assume that the initial pdf for $\boldsymbol{\xi}$ to be a standard pdf (such as standard normal). Construct the polynomial chaos expansion by finding the coefficients a_j, such that

$$\boldsymbol{\theta}_k = \sum_{j=0}^{P} a_j \Psi(\boldsymbol{\xi}_{k_j}). \tag{34}$$

   Here, the orthogonal polynomial functions $\{\Psi(\boldsymbol{\xi})\}$ are selected from the Askey scheme.

2. The projections b_j in Eq. (33) are computed using Eq. (28). This serves as a surrogate for the forward problem.

3. Simulate N samples of $\{\boldsymbol{\xi}_{k_i}\}_{i=1}^{N}$.

4. For $k = 1$, the prior predictions $\boldsymbol{\xi}_k^*$ are calculated from the forward problem by substituting $\{\boldsymbol{\xi}_{k_i}\}_{i=1}^{N}$ in Eq. (33).

5. The remaining steps are identical to the steps in section 2.1.

Approach 2 is computationally cheaper as it avoids construction of PCE at every time step of filtering and uses the chaos coefficients calculated at the initial time step to bypass the computation of the function $\mathbf{g}_k(\,\cdot\,)$ in Eq. (6). However, there is a need for caution. The drawback in this approach is that at each time step, the pdf of the primary random variables $\boldsymbol{\xi}$ change. However, in the PCE representations used in Eqs. (33-34) the same set of orthogonal polynomials $\{\Psi_i\}$ and the corresponding projections are used. Clearly, this leads to a suboptimal situation in terms of convergence and may require a larger number of terms in the expansion [43]. These difficulties can be overcome by adopting either of the two simple procedures:

(a) The series expansions may be truncated after $J >> P$ terms so that series convergence need not be a serious issue,

(b) A new PCE expansion is carried out after T iterations.

The above two correcting procedures have been implemented together to improve the efficiency of the algorithm without adversely affecting the computational efficiency too much. The proposed method is demonstrated through two numerical examples. These are presented in the following section.

5 Numerical Examples and Discussions

A set of numerical examples are presented to demonstrate the applicability and performance of the proposed method. First, the problem of parameter identification in a Duffing oscillator is considered. Subsequently, we consider the parameter identification problem in an oscillating airfoil in unsteady flow. In both these examples, the measurements have been synthetically generated by solving the forward problem and adding synthetic noise to the time histories of the response. This is used as an input for the system identification algorithm. In both these problems, the system response is expressed as a PCE whose coefficients have been determined using the non-intrusive probabilistic collocation method. This method is shown to be computationally efficient especially when the nonlinearity is significant such as in the fluid-structure interaction problem considered in the second example [45]. Once the PCE of the unknown parameters and the solution of the forward problem have been established, the implementation of the BFA has been carried out in the transformed variable space using the method outlined in section 4.2.

To demonstrate the efficiency of the proposed method, the numerical results have been presented when (A) BFA is applied without PCE, and (B) when BFA is applied with PCE. To investigate further avenues for reducing the computational costs associated with implementation of the algorithm, we have considered the following four methods:

(a) **Method 1**: This involves implementing the BFA at all available measurement points. Figure 1 shows a schematic of Method 1. The circles represent data points and the likelihood L_i are calculated at each measurement point. Thus, if M data points are available and filtering is carried out with N particles at each measurement, this method would require $(N \times M)$ solutions of the forward problem.

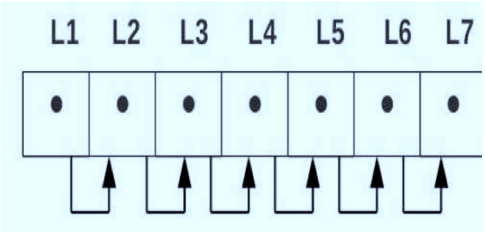

Fig. 1 Schematic of Method 1.

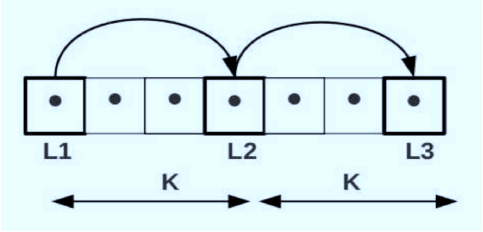

Fig. 2 Schematic of Method 2.

(b) **Method 2**: In this method, the BFA is applied at every K measurement points, resulting in $(N \times M)/K$ solutions of the forward problem; see Fig. 2 for a schematic. In this method all the information available about the system through the measurements is not used which effectively implies inefficient usage of available information.

(c) **Method 3**: As in Method 2, the particle filtering is carried out every K measurement points. However, the likelihood function for $\boldsymbol{\theta}_k$ is now computed in a different way. For all the measurement data points between t_k and t_{k+K}, the likelihood L_i are computed for $\boldsymbol{\theta}_k$. A mean likelihood is computed as $\bar{L} = \sum_{i=1}^{K} L_i$, which is used as the prior density function for resampling of $\boldsymbol{\theta}$ at time step t_{k+K}. The method is explained through the schematic shown in Fig. 3. It

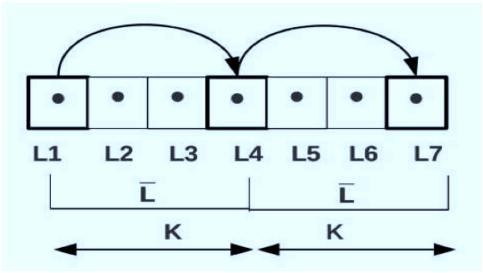

Fig. 3 Schematic of Method 3.

must be emphasized here that computation of the likelihoods L_i for time steps $t_k, t_{k+1}, \ldots, t_{k+K}$ can be computed directly by solving the forward problem for a given realization of $\boldsymbol{\theta}$ corresponding to time t_k. Thus, even though the number of solutions of the forward problem is $(N \times M)/K$, unlike in Method 2, no available information is wasted. The computational costs involved in computing the likelihoods for all time steps $t_k, t_{k+1}, \ldots, t_{k+K}$ is marginal.

(d) **Method 4**: This is another variant of Method 2 where the filtering is carried out every K steps. Here, the measurements $y_k, y_{k+1}, \ldots, y_{k+K}$ are replaced by its mean value $\bar{y} = \sum_{i=1}^{K} y_{k+i}$ based on which the likelihood L_i are calculated at each K th measurement point. Figure 4 provides a schematic for this method. This method also requires $(N \times M)/K$ evaluations of the forward problem. However, the computational costs would be less than in Method 2 as the likelihoods L_i are now evaluated only at the filtering points. Clearly, this method would work well as long as the dynamics of the system do not get appreciably altered within K measurement points and is expected to work well where noise in the measurements is significant.

For the sake of simplicity, the model and the measurement noise are assumed to be Gaussian white noise processes. Though white noise models are physically unrealizable, assuming noise to be white is acceptable when the correlation length of the noise process is negligible in comparison to the correlation length of the system response. This is usually

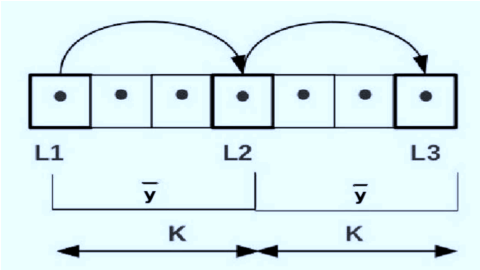

Fig. 4 Schematic of Method 4.

true if the oscillations in the noise are significantly faster than those exhibited by the dynamical system. Under these assumptions, the time discretized noise processes $\mathbf{w}_k$ and $\mathbf{v}_k$ constitute a sequence of vectors of i.i.d. random variables. Moreover, in these numerical examples, it is assumed that the system parameters to be identified do not change within the small period of time when the measurements are being recorded. Since the system parameters remain time invariant, it is obvious that in the discretized recursive format, $\boldsymbol{\theta}_{k+1} = \boldsymbol{\theta}_k$. However, in writing the model equation, a model noise is added such that the model equation can now be written as

$$\boldsymbol{\theta}_{k+1} = \boldsymbol{\theta}_k + \mathbf{w}_k. \tag{35}$$

Here, $\mathbf{w}_k$ is an artificial noise and does not have any physical significance. The reasons for adding $\mathbf{w}_k$ are numerical and is explained next.

In the implementation of the BFA, in subsequent iterations the samples are generated from the normalized likelihood function. In the absence of noise $\mathbf{w}_k$, the population of the samples would be limited to the sample set that have been generated at $k = 0$. This leads to the following difficulties:

(a) After a few iterations, all the samples generated for $\boldsymbol{\theta}_{k+1}$ would be identical leading to a degenerate condition resulting in the breakdown of the algorithm, and

(b) the accuracy of the system parameter estimates would depend on the closeness of the initial set of variables generated at $k = 0$ to the actual system parameters. Thus, the accuracy of the method is left to chance.

To prevent such degeneracies, the artificial model noise $\mathbf{w}_k$ is added to the posterior estimates of $\boldsymbol{\theta}_k$, at each iteration. This leads to a jittering of the samples in the population and ensures that the samples are different from the set of samples at the preceding iteration step. It is reasonable to assume that $\mathbf{w}_k$ is independent of time as well as $\boldsymbol{\theta}_k$ and $\mathbf{v}_k$. Usually, a Gaussian model for $p(\mathbf{w}_k)$ can be assumed with zero mean and a small variance. The variance should be small so that the population of samples generated from the probability mass function are slightly different from the samples that have been identified as having higher likelihoods. Also, this enables generation of a larger number of samples around the most likely sample, leading to the possibility of achieving greater accuracy levels.

5.1 Example 1: Harmonically excited Duffing oscillator

A Duffing oscillator subjected to harmonic loading is considered. The governing equation of motion is given by

$$m\ddot{x} + c\dot{x} + kx + k_1 x^3 = \gamma \cos(\omega t), \tag{36}$$

where, the parameters are assumed to have the following nunerical values: $m = 10$, $c = 25$, $k = 100$, $k_1 = 100$, $\gamma = 100$ and $\omega = \pi$ rad/s. The measurements are synthetically generated by numerically integrating Eq. (36) and adding a Gaussian noise with 1% variance. The sampling rate of the measurements is assumed to be $100\ \mathrm{s}^{-1}$. Figure 5 shows the time history of the response and the synthetically generated noisy measurements.

5.1.1 Case A: Only one unknown parameter

Initially, it is assumed that only the nonlinear stiffness k_1 is unknown. The prior density for k_1 is assumed to be Gaussian $\sim \mathcal{N}(90, 10)$. First, a PCE representation of the response is constructed where P is taken to be 2, n is 1 and n_p is 2. A comparison of the mean response obtained from PCE and that obtained from Monte-Carlo simulations (MCS) are shown in Fig. 6. An exact match is observed indicating the acceptability of the PCE representation. The number of forward evaluations required for constructing the PCE is 4.

In the application of BFA, $N = 200$ particles are considered at each iteration. Figures 7-10 illustrate the predictions obtained using Methods 1-4. In applying Methods 2-4, K is taken to be 25. A summary of the performance of the four methods in terms of computational costs is presented in Table 1. It is seen that while BFA without PCE requires 1001×200 solutions of the forward problem, combining PCE with the filter requires only 4 calls to the forward problem. The computational costs when PCE is used, reduces significantly ranging from 10 times to 40 times for Methods 1-4. For more complicated problems where the solution of a single forward problem is time consuming, the savings in computational costs can be even more considerable. The accuracy levels observed for Methods 2-4 are similar to that obtained from Method 1.

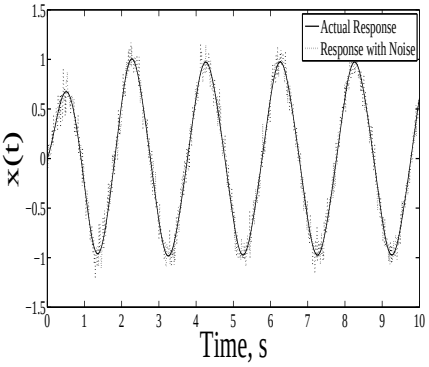

Fig. 5 Time history of response seeded with noise

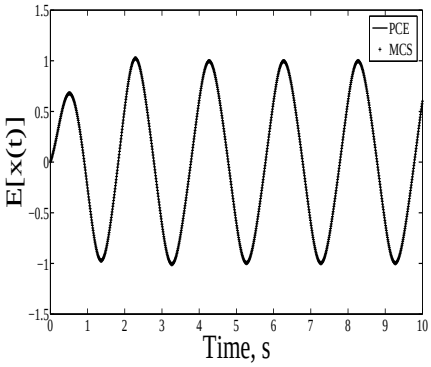

Fig. 6 Comparison of response using PCE and MCS

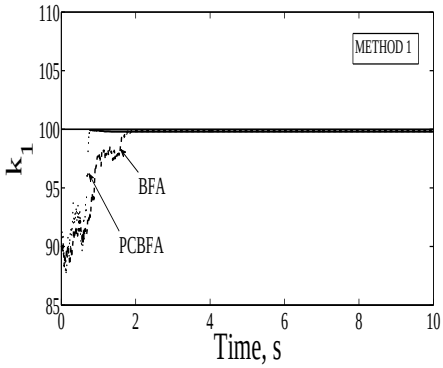

Fig. 7 Example 1 A: Estimates of stiffness using Method 1.

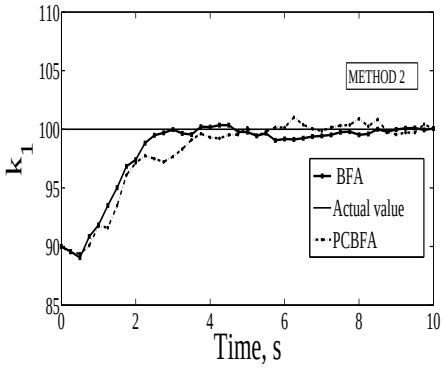

Fig. 8 Example 1 A: Estimates of stiffness using Method 2.

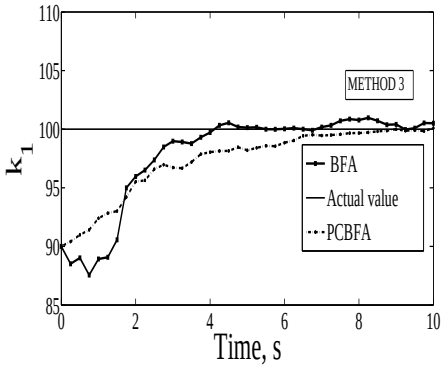

Fig. 9 Example 1 A: Estimates of stiffness using Method 3.

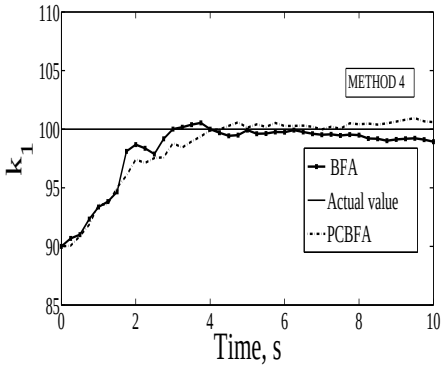

Fig. 10 Example 1 A: Estimates of stiffness using Method 4.

Method	A	B	C	D	E	F
Method 1	PCBFA	1001	4	99.78	-0.22	24.67
	BFA	1001	200200	99.81	-0.19	1003.1
Method 2	PCBFA	40	4	100.15	0.15	2.68
	BFA	40	8000	99.879	-0.121	46.04
Method 3	PCBFA	40	4	99.52	-0.48	6.11
	BFA	40	8000	100.4	0.40	45.90
Method 4	PCBFA	40	4	100.35	0.35	3.13
	BFA	40	8000	99.366	-0.634	45.83

Table 1 Example 1 A: Comparison of performance; A = Methodology; B = Number of filtering iterations; C = Number of solutions of the forward problem; D = Mean of the estimate; E = $\%$ Error; F = CPU time in seconds.

5.1.2 Case B: Two unknown parameters

Next, the problem is repeated when the nonlinear stiffness k_1 and damping c are assumed to be unknown. With n = 2 and assuming 3rd order polynomials in the PC expansion, the value of P is 9. However, since the focus is on representing the response only for about 40 s, with about 20 cycles, it was found that a good match with MCS was obtained even when P was taken to be 6. In this study, we have considered $P = 6$ so as to keep the number of random variables to as low a value as possible. The comparison of the mean response obtained from MCS with the PCE containing 6 terms is shown in Fig. 11, indicating a good match. The time histories of the first few random modes of the response are plotted in Figs. 12-13. The zeroth order mode, a_0, is the mean, which has the most significant contribution to the final solution. a_1, a_2, a_3 are the higher order random modes. It is clear from Figs. 12-13, that a decrease in P does not affect the response calculations significantly.

Methods 1 -4 are used to estimate the two unknown parameters. In application of the filter, $N = 500$ particles have been used. The results of the predictions for k_1 and c are shown in Figs. 14-17 and Figs. 18-21 respectively. Table 2 provides a comparison of the predictions and the associated computational costs.

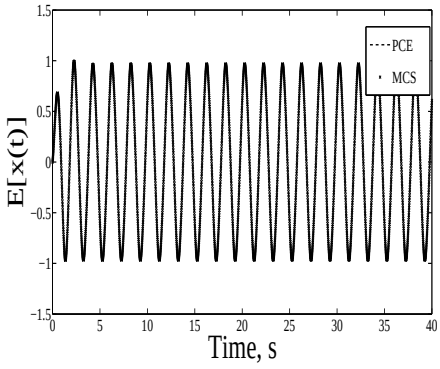

Fig. 11 Comparison of response using PCE and MCS

In method 1, as seen from Table 2, the PCE based approach involves 64 number of structural analyses, while ordinary BFA requires 4001×500 solutions of the forward problem. It can be seen that the PCE based approach is nearly 13 times faster than the ordinary BFA for the same level of accuracy in both the estimates. In methods 2-4, the algorithm is processed at every 50 time steps. As expected, the approach of implementing BFA at regular intervals in these three methods yielded much faster estimates on compared to method 1. The PCE based approaches are found to be roughly 12 times faster than ordinary BFA. Despite yielding faster estimates in these three methods, the estimates obtained through PCE based approaches are still found to be in good agreement with the actual values of the two unknown parameters. This proves the effectiveness of the algorithm in identifying multiple system parameters with reasonable accuracies.

5.2 *Example 2: Oscillating Airfoil in an Unsteady Flow*

We next consider a highly nonlinear fluid-structure interaction problem of an oscillating airfoil in an unsteady flow. The airfoil is modeled as a $2D$ system having degrees of freedom along the pitching and heaving directions; see Fig. 22 for a schematic diagram of the system. Assuming that the plunging deflection is denoted by h, positive in the downward

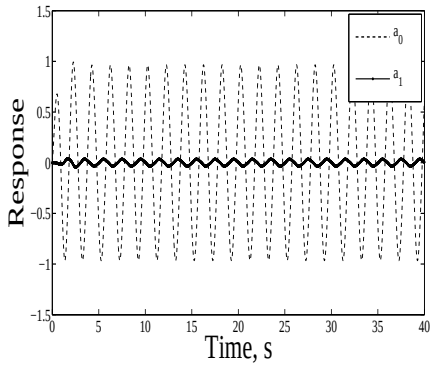

Fig. 12 Time history response of the first two random modes.

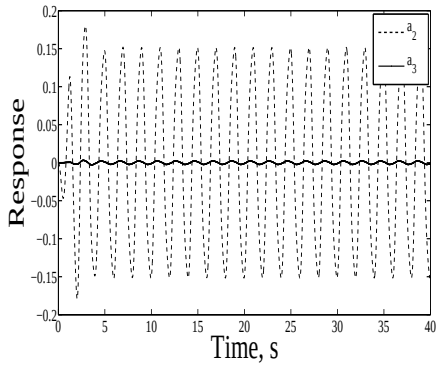

Fig. 13 Time history response of the 3rd and 4th random modes.

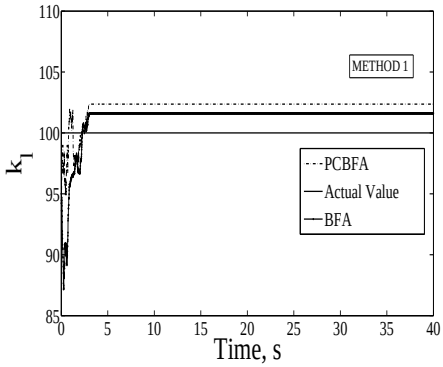

Fig. 14 Example 1 B: Estimates of stiffness using Method 1.

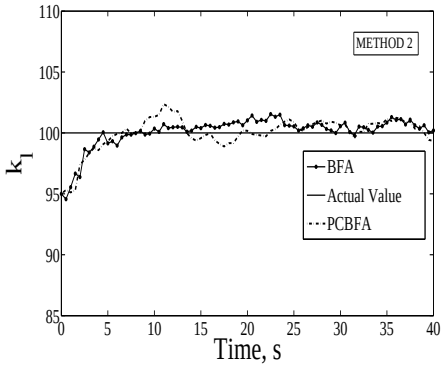

Fig. 15 Example 1 B: Estimates of stiffness using Method 2.

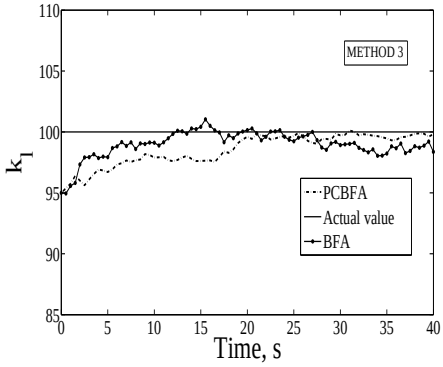

Fig. 16 Example 1 B: Estimates of stiffness using Method 3.

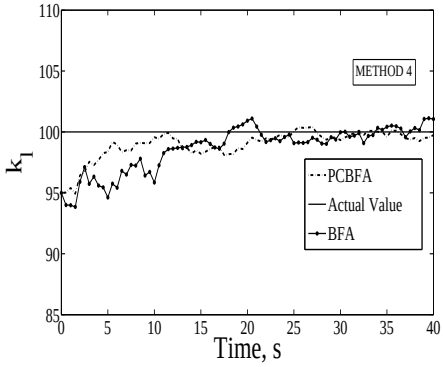

Fig. 17 Example 1 B: Estimates of stiffness using Method 4.

direction, and the pitching angle by α, taken to be positive with nose up, the aero-elastic equations are given by the following coupled integro-differential equations [46]

$$\epsilon'' + x_\alpha \alpha'' + 2\zeta_\epsilon \frac{\overline{\omega}}{U}\epsilon' + (\frac{\overline{\omega}}{U})^2(\epsilon + \beta_\epsilon \epsilon^3) = -\frac{1}{\pi\mu}C_L(\tau), \tag{37}$$

$$\frac{x_\alpha}{{r_\alpha}^2}\epsilon'' + \alpha'' + 2\frac{\zeta}{U}\alpha' + \frac{1}{U^2}(\alpha + \beta_\alpha \alpha^3) = \frac{2}{\pi\mu {r_\alpha}^2}C_M(\tau). \tag{38}$$

Here, $\epsilon = h/b$ is the non-dimensional plunge displacement of the elastic axis, β_ϵ and β_α are the nonlinear spring constants, r_α is the radius of gyration about the elastic axis, $a_h b$ denotes the distance of the elastic axis from the mid chord and $x_\alpha b$ is the distance of the mass center from the elastic axis, ζ_ϵ and ζ_α are the damping ratios in plunge and pitch respectively, U is

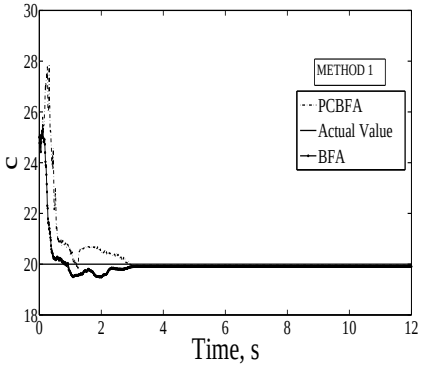

Fig. 18 Example 1 B: Estimates of damping using Method 1.

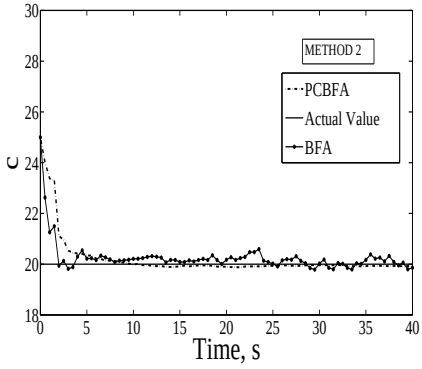

Fig. 19 Example 1 B: Estimates of damping using Method 2.

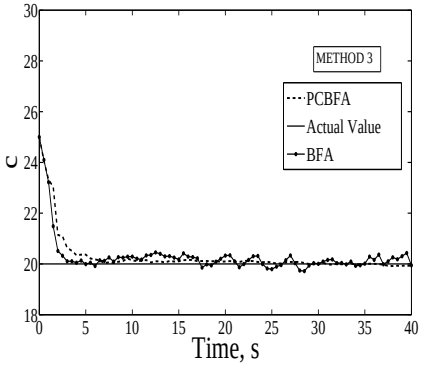

Fig. 20 Example 1 B: Estimates of damping using Method 3.

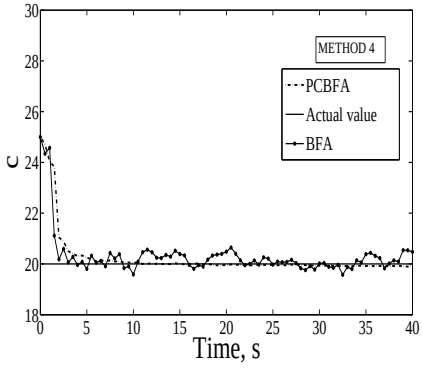

Fig. 21 Example 1 B: Estimates of damping using Method 4.

Method	A	B	C	D	E	F	G	H
Method 1	PCBFA	4001	64	102.4	2.4	19.95	-0.25	884.2
	BFA	4001	2000500	101.62	1.62	19.91	-0.45	11142
Method 2	PCBFA	80	64	100.43	0.43	19.93	-0.35	21.09
	BFA	80	40000	100.6	0.6	20.1	0.5	263.4
Method 3	PCBFA	80	64	99.57	-0.43	20.02	0.1	120.7
	BFA	80	40000	99.14	-0.86	20.07	0.35	271.17
Method 4	PCBFA	80	64	99.63	-0.37	19.93	-0.35	22.42
	BFA	80	40000	99.9	-0.10	20.12	0.6	265.16

Table 2 Example 1 B: Comparison of the performance; A = Methodology; B = Number of times BFA is implemented; C = Number of solutions for forward problem; D = Mean of the estimate,k_1; E = $\%$ Error in k_1; F = Mean of the estimate,c; G = $\%$ Error in c; H = CPU time in seconds.

the non-dimensional stream velocity given by $U = v/(b\omega_\alpha)$, $\overline{\omega} = (\omega_\epsilon/\omega_\alpha)$, where, ω_ϵ and ω_α are respectively the natural frequencies of the uncoupled plunging and pitching modes and $\tau = vt/b$ is the non-dimensional time. The exponent $(\,\cdot\,)'$ denotes differentiation with respect to non-dimensional time τ. For incompressible, inviscid unsteady flow, the lift and pitching moment coefficients are expressed as $C_L(\tau)$ and $C_M(\tau)$ in Eqs. (37-38) and are given by [47]

$$\begin{aligned} C_L(\tau) &= \pi(\epsilon'' - a_h\alpha'' + \alpha') + 2\pi\{\alpha(0) + \epsilon'(0) + [\frac{1}{2} - a_h]\alpha'(0)\}\phi(\tau) \\ &\quad +2\pi\int_0^T \phi(\tau-\sigma)[\alpha'(\sigma)\epsilon''(\sigma) + [\frac{1}{2} - a_h]\alpha''(\sigma)]\mathrm{d}\sigma, \end{aligned} \tag{39}$$

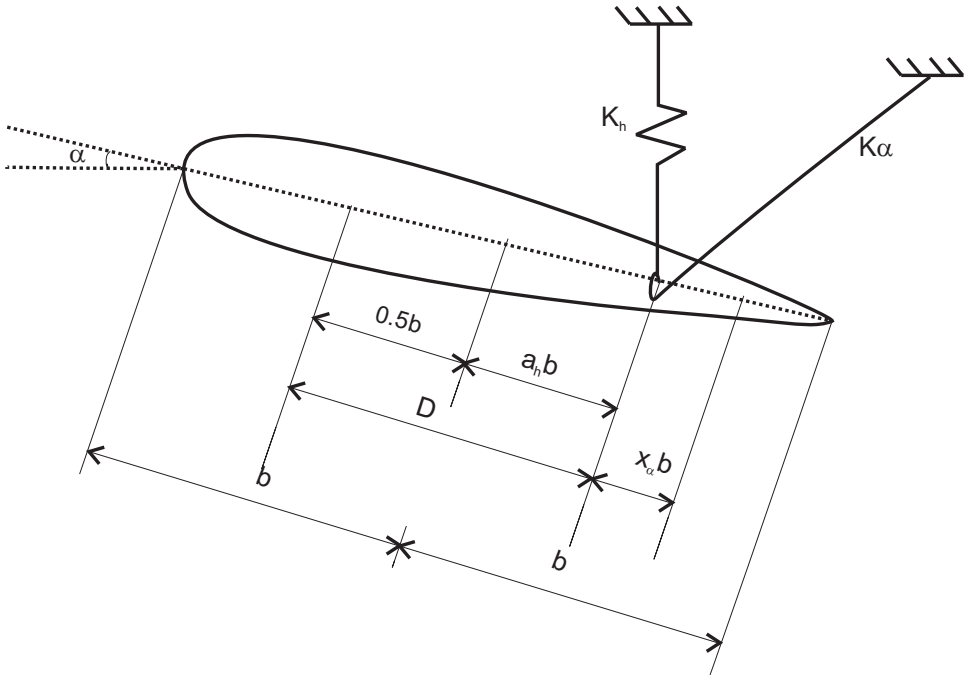

Fig. 22 Schematic diagram of a 2-D airfoil.

$$\begin{aligned} C_M(\tau) &= \pi[\frac{1}{2}+a_h]\times\{\alpha(0)+\epsilon'(0)+[\frac{1}{2}-a_h]\alpha'(0)\}\phi(\tau) \\ &\quad +\pi[\frac{1}{2}+a_h]\times\int_0^T\phi(\tau-\sigma)\{\alpha'(\sigma)+\epsilon''(\sigma)+[\frac{1}{2}-a_h]\alpha''(\sigma)\}\mathrm{d}\sigma \\ &\quad +\frac{\pi}{2}a_h(\epsilon''-a_h\alpha'')-[\frac{1}{2}-a_h]\frac{\pi}{2}\alpha'-\frac{\pi}{16}\alpha''. \end{aligned} \tag{40}$$

Here, $\epsilon(0)$, $\epsilon^{'}(0)$, $\alpha(0)$ and $\alpha^{'}(0)$ respectively denote the initial conditions, $\phi(\tau)$ is the Wagner function expressed as

$$\phi(\tau) = 1-\psi_1 e^{-\epsilon_1\tau}-\psi_2 e^{-\epsilon_2\tau} \tag{41}$$

and the constants $\psi_1 = 0.165$, $\psi_2 = 0.355$, $\epsilon_1 = 0.0455$ and $\epsilon_2 = 0.3$ are as reported in [46]. Equations (37-40) collectively represents the governing equations for the oscillating airfoil and represents a highly nonlinear fluid structure interaction problem. The nonlinearity in these equations arise not only due to the structural nonlinearities but also on account of the fluid-structure interaction effects. The numerical solution of this forward problem has been discussed in the literature; these details are presented in the Appendix for the sake of completeness.

We now assume that the nonlinear stiffness coefficients, β_ϵ and β_α to be the parameters that are to be identified from measurements of the response. Both these parameters were assumed to have Gaussian prior densities $\mathcal{N}(4, 0.5)$. The numerical values of the remaining parameters were assumed to be as follows: μ = 100, $\overline{\omega} = 0.2$, $a_h = -0.5$, $x_\alpha = 0.25$, $\zeta_\alpha = 0$, $\zeta_\epsilon = 0$, $r_\alpha = 0.5$. To synthetically generate the measurements, the unknown parameters β_α and β_ϵ were both assumed to be 3.5. The analysis is performed assuming $U = 6.8$. Time histories of the pitching and the heaving motions were obtained from numerical integration of Eqs. (37-38). The time history of the pitching response was assumed to be the measurements which serve as the input to the filtering algorithm. To synthesize the measurements, the computed time history, obtained for 600 dimensionless time units, was added with a zero mean Gaussian noise of 1% variance.

In application of PCBFA, a PCE for the response needs to be constructed. Using the probabilistic collocation technique, a 9 term expansion has been constructed for the response. A comparison of the time history of the mean response obtained by numerical integration(MCS) and PCE is shown in Fig. 23. Some degeneracy in the PCE response is observed from 300 s. However, this is not significant; more discussions on this is available later in the paper. A representative pdf of the response calculated at $t = 190$, is shown in Fig. 24. Both the figures show a reasonable good match for the results obtained from PCE and MCS, indicating satisfactory PCE construction of the system.

The application of the filtering algorithm was considered with 500 particles at each iterate. As in the previous example, the results were obtained using Methods 1-4. In application of Methods 2-4, K was taken to be 25. The results of the

predictions for β_α and β_ϵ are shown in Figs. 25-32. The summary of the analysis by all the four methods has been shown in Table 3.

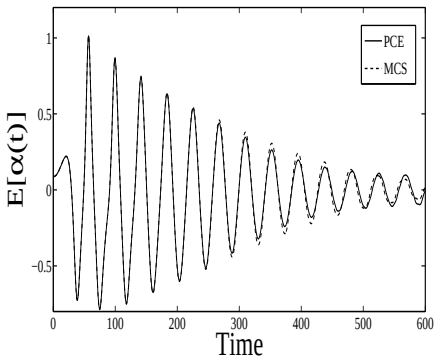

Fig. 23 Example 2: Comparison of response using PCE and MCS

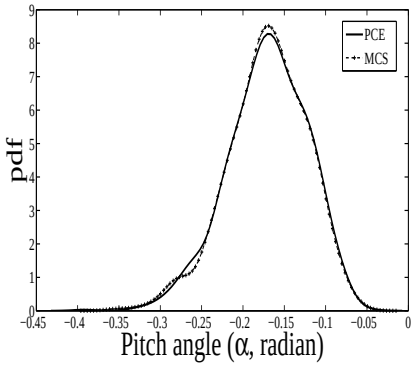

Fig. 24 Example 2: Comparison of pdf of response using PCE and MCS

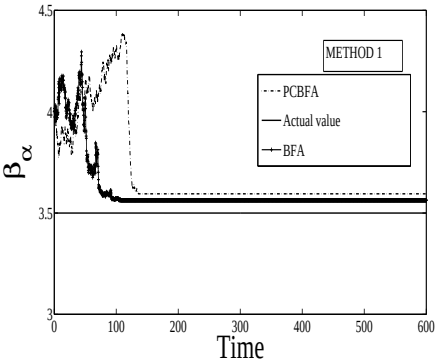

Fig. 25 Example 2: Estimates of β_α using Method 1.

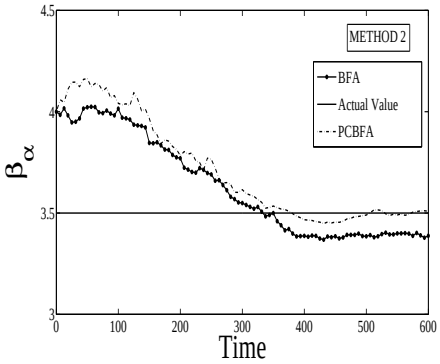

Fig. 26 Example 2: Estimates of β_α using Method 2.

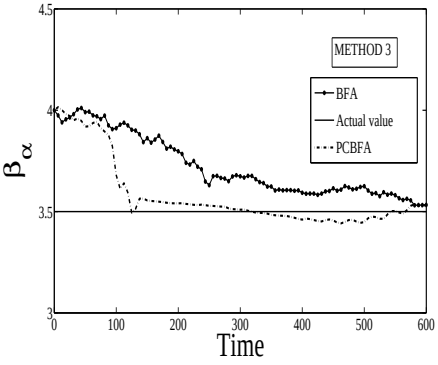

Fig. 27 Example 2: Estimates of β_α using Method 3.

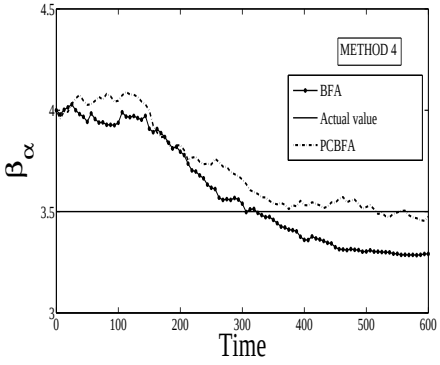

Fig. 28 Example 2: Estimates of β_α using Method 4.

A comparison of the errors in the estimates of the unknown parameters reveal that consistently, the proposed method PCBFA leads to marginally better estimates in comparison to BFA. More importantly, the number of forward evaluations required is only a small fraction in comparison to BFA. The consequent acceleration in the application of the filtering algorithm is evident from the computational times required in the two approaches. It is also worth noting that the proposed method, PCBFA, is significantly faster when Methods 2-4 are employed where one does not make use of all the available measurements. When a comparison is made between Methods 3 and 4, it is surprising to observe that the errors in Methods 3 and 4 are of the same order. However, if K is taken to be large, it is expected that the performance of Method 4 would

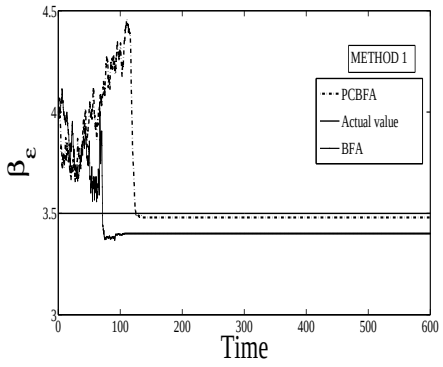

Fig. 29 Example 2: Estimates of β_ϵ using Method 1.

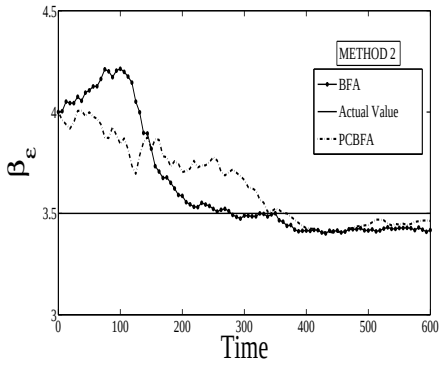

Fig. 30 Example 2: Estimates of β_ϵ using Method 2.

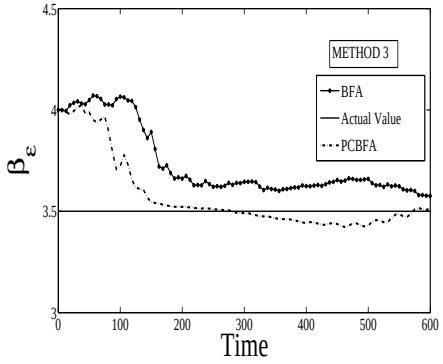

Fig. 31 Example 2: Estimates of β_ϵ using Method 3.

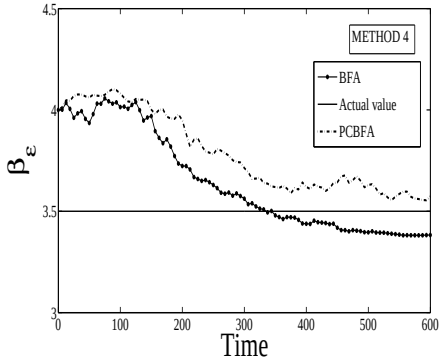

Fig. 32 Example 2: Estimates of β_ϵ using Method 4.

Method	A	B	C	D	E	F	G	H
Method 1	PCBFA	2401	100	3.6	2.85	3.48	-0.57	210.3
	BFA	2401	1200000	3.56	1.71	3.40	-2.85	6856.4
Method 2	PCBFA	96	100	3.49	-0.28	3.45	-1.42	11.95
	BFA	96	48000	3.39	-3.14	3.42	-2.28	281.19
Method 3	PCBFA	96	100	3.48	-0.57	3.46	-1.14	40.3
	BFA	96	48000	3.56	1.71	3.61	3.14	289.17
Method 4	PCBFA	96	100	3.55	1.42	3.63	3.71	16.8
	BFA	96	48000	3.38	-3.42	3.42	-2.28	288.5

Table 3 Example 2: Comparison of the performance of Methods 1-4; A = Methodology; B = Number of times BFA is implemented; C = Number of structural analyses; D = Mean of the estimate,β_α; E = $\%$ Error in β_α; F = Mean of the estimate,β_ϵ; G = $\%$ Error in β_ϵ; H = CPU time in seconds.

deteriorate. Interestingly, even though the number of solutions of the forward problem are the same in the Methods 2-4, the computational effort in Method 3 is higher by about 50% due to the additional computations required in estimating the likelihoods at all the measurement data points. This has been observed consistently in all the numerical problems.

6 Concluding Remarks

A numerical algorithm has been developed for identifying the system parameters in a nonlinear dynamical system from noisy measurements of the response. The proposed algorithm is based on the bootstrap particle filter algorithm available in the literature. This involves recursively updating the prior density of the system parameters as more measurements become available using Bayesian principles and an estimate of the parameters is obtained by computing the first moment. A major drawback of the bootstrap particle filter algorithm is the requirement of solving the forward problem a large number of

times as this places severe constraints on the computational costs, especially for complicated dynamical systems with large nonlinearities. The developments proposed in this paper can be used to accelerate the filtering algorithm by reducing the number of times the forward problem needs to be solved. The salient features arising from this study can be summarized as follows:

1. A polynomial chaos based approach has been integrated with the bootstrap particle filter algorithm. This involves constructing the PCE for the response of the dynamical system, which is subsequently used in particle filtering.
2. The PCE for the response is constructed at the initial time step and the problem of system identification is subsequently formulated in the space of the random variables spanned by the orthogonal polynomials used in PCE. This implies a transformation of the system identification problem to the space spanned by these random variables and eliminates the need for construction of PCE for the response at each time step.
3. Issues related to the convergence of the PCE due to changes in the probability density function of the random variables which form the support of the orthogonal polynomials can be bypassed by considering a larger number of terms in the PC expansion. To illustrate this, a PC expansion with 20 terms was constructed in the airfoil problem. A comparison of the mean response obtained from PCE and MCS is shown in Fig. 33. Here, the convergence in the PCE response is significantly better than when 9 terms had been used (see Fig. 23); the degeneracy appears only after 500 s. On performing the identification using the 20 term PCE response, similar level of accuracy in the estimates was seen; see Fig. 34. A comparison of the corresponding parameter identification as shown in Fig. 27 reveals that the convergence

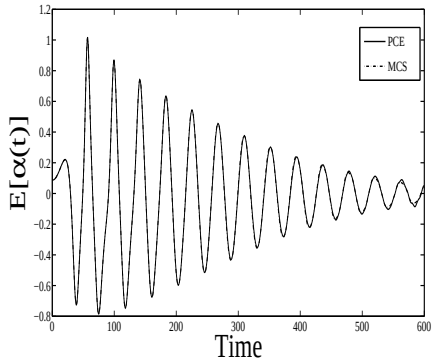

Fig. 33 Comparison of mean response with 20 term PCE and MCS

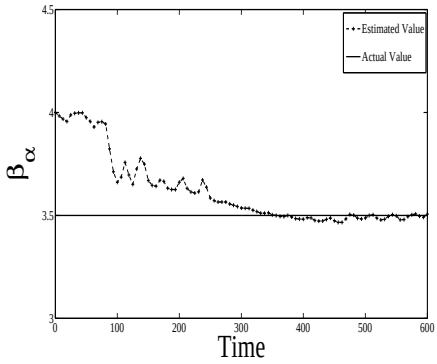

Fig. 34 Estimate of β_α using Method 3 with 20 term PCE

in the identification of the parameter is faster when higher number of PCE terms are considered. However, the accuracy levels of the identified parameters remain comparable.

4. A reduction in the dimension of the size of the variables on which the system identification is carried out is achieved by rewriting the model and the measurement equations in a form different from the convention. This has earlier been proposed in [35]. The proposed developments in the bootstrap filter algorithm in conjunction with PCE maintains this dimension reduction.
5. Secondary measures of reduction in computational effort has been investigated. Three such methods, which bypass the need for application of the filter algorithm at all measurement points have been studied. Methods which do not ignore completely all the measurements have been observed to be more accurate but at a marginally greater computational cost.
6. The methods developed in this paper have been implemented to identify the parameters of a nonlinear oscillator and in a highly nonlinear fluid-structure interaction problem. The proposed method has been observed to lead to fairly accurate estimates of the parameters at a fraction of the computational costs in comparison to the bootstrap particle filter available in the literature. This holds promise that the method can be used for system identification in large scale dynamical systems.
7. Since the focus of the studies carried out in this paper has been on developing strategies for accelerating the particle filter and observing its efficiency, no efforts have been made to use strategies such as sequential importance sampling for achieving faster convergence as this can be separately applied to both BFA and PCBFA. For similar reasons, no effort has been made to use smoothening techniques to reduce the statistical fluctuations in the estimates of the mean for the parameters being identified.

8. Identification of system parameters using the proposed method for nonlinear dynamical systems exhibiting chaos may not be feasible. More studies need to be undertaken before one can comment on this issue.

Finally, it must be emphasized here that particle filtering has been traditionally used in the literature for real time dynamic state estimation. However, this is not a necessary constraint. Here, it is proposed to use particle filtering for system identification from vibration measurements in structural systems but not in real time. System identification is the first step in any structural health monitoring strategies where damage indicators are first identified and a prognosis is made about their progress which are subsequently monitored.

Acknowledgement
This work was partially supported from the project sponsored under the National Program on Micro and Smart Systems (NPMASS), Aeronautical Development Agency, Government of India.

A Appendix: Solution of the Aeroelastic Problem

The governing equations of motion in Eqs. (37-40) represent a set of coupled integro-differential equations which are difficult to numerically integrate in this form. A technique by which these equations can be transformed to a form amenable for numerical integration has been discussed in [46]. For the sake of completeness, a summary of this approach is presented here.

The state variables of the integro-differential equations comprise of the following parameters α, $\alpha^{'}$, ϵ and $\epsilon^{'}$, where, the superscript $(^{'})$ has the same meaning as in Eqs. (37-40). The state space $\mathbf{X} = \{\alpha, \alpha', \epsilon, \epsilon', w_1, w_2, w_3, w_4\}$ is augmented using four additional state variables, given by,

$$\begin{aligned} w_1 &= \int_0^T e^{-\epsilon_1(\tau-\sigma)}\alpha(\sigma)\,\mathrm{d}\sigma, \\ w_2 &= \int_0^T e^{-\epsilon_2(\tau-\sigma)}\alpha(\sigma)\,\mathrm{d}\sigma, \\ w_3 &= \int_0^T e^{-\epsilon_1(\tau-\sigma)}\epsilon(\sigma)\,\mathrm{d}\sigma, \\ w_4 &= \int_0^T e^{-\epsilon_2(\tau-\sigma)}\epsilon(\sigma)\,\mathrm{d}\sigma. \end{aligned} \tag{42}$$

Equations (37-40) can now be recast into the first order form $X' = f(X)$, where, $X = \{x_1, x_2, x_3, x_4, x_5, x_6, x_7, x_8\} = \{\alpha, \alpha', \epsilon, \epsilon', w_1, w_2, w_3, w_4\}$. Explicitly, this can be expressed as

$$\begin{aligned} x_1' &= x_2, \\ x_2' &= \frac{c_0 N - d_0 M}{c_1 d_0 - c_0 d_1} \\ x_3' &= x_4 \\ x_4' &= \frac{-c_1 N + d_1 M}{c_1 d_0 - c_0 d_1} \\ x_5' &= x_1 - \epsilon_1 x_5 \\ x_6' &= x_1 - \epsilon_2 x_6 \\ x_7' &= x_3 - \epsilon_1 x_7 \\ x_8' &= x_3 - \epsilon_2 x_8, \end{aligned} \tag{43}$$

where,

$$\begin{aligned} M &= c_2 x_4 + c_3 x_2 + c_4 x_3 + c_5 x_3^3 + c_6 x_1 \\ &\quad + c_7 x_5 + c_8 x_6 + c_9 x_7 + c_{10} x_8 - f(\tau), \\ N &= d_2 x_2 + d_3 x_1 + d_4 x_1^3 + d_5 x_4 + d_6 x_3 \\ &\quad + d_7 x_5 + d_8 x_6 + d_9 x_7 + d_{10} x_8 - g(\tau). \end{aligned} \tag{44}$$

The coefficients $c_0..c_{10}$ and $d_0..d_{10}$ depend on the system parameters, and their expressions along with $f(\tau)$ and $g(\tau)$ are as follows:

$$\begin{aligned} f(\tau) &= \frac{2}{\mu}((\frac{1}{2}-a_h)\alpha(0)+\epsilon(0))(\psi_1\epsilon_1 e^{-\epsilon_1\tau}+\psi_2\epsilon_2 e^{-\epsilon_2\tau}), \\ g(\tau) &= -\frac{(1+2a_h)f(\tau)}{2{r_\alpha}^2}. \end{aligned} \tag{45}$$

References

[1] R.E. Kalman, A new approach to linear filtering and prediction problems, Journal of Basic Engineering D ASME, **82**, 35-45 (1960).
[2] L. Ljung, Asymptotic behavior of the extended Kalman filter as a parameter estimation for linear systems, Proceedings IEEE AC, **24**, 36-50 (1979).
[3] M. Hoshiya and E. Saito, Structural identification by extended Kalman filter, Journal of Engineering Mechanics ASCE, **110**, 1757-1770 (1984).
[4] M. Shinozuka, C.B. Yum and H. Imai, Identification of structural dynamic systems, Journal of Engineering Mechanics Division ASCE, **108**, 1371-1390 (1982) .
[5] R. Ghanem and M. Shinozuka, Structural system identifcation I: Theory, Journal of Engineering Mechanics ASCE, **121**(2), 255-264 .
[6] J. Li and J.B. Roberts, Stochastic structural system identification, Computational Mechanics, **24**, 206-(1999) .
[7] D. Wang and A. Haldar, System identification with limited observations and without input, Journal of Engineering Mechanics ASCE, **123**(5), 504-511 (1997) .
[8] E.A. Wan and R V.D. Merwe, The unscented Kalman filter for nonlinear estimation, Adaptive Systems for Signal Processing, Communications and Control Symposium IEEE, 153-158 (2000).
[9] Y. Chen and D. Zhang, Data assimilation for transient flow in geologic formations via ensemble Kalman filter, Advances in Water Resources, **29**, 1107-1122 (2006).
[10] R. Tipireddy, H.A. Nasrellah and C.S. Manohar, A Kalman filter based strategy for linear structural system identification based on multiple static and dynamic test data, Probabilistic Engineering Mechanics, **24**, 60-74 (2009).
[11] F. Abid, G. Chevallier, J.L. Blanchard, J.L. Dion and N. Dauchez, System identification using Kalman filters, Proceedings of the 31st IMAC 7 561-573 (2014).
[12] M. Evans and T. Swartz, Methods for approximating integrals in statistics with special emphasis on Bayesian integration problems, Statistical Science, **10**(3), 254-272 (1995) .
[13] R. Cools and P. Dellaportas, The role of embedded integration rules in Bayesian statistics, Statistics and Computing, **6**, 245-260 (1996).
[14] M. Evans and T. Swartz, Approximating integrals via Monte Carlo and deterministic methods, (Oxford University Press, 2000).
[15] N.J. Gordon, D.J. Salmond and A.F.M. Smith, Novel approach to nonlinear/non-Gaussian Bayesian state estimation, IEE Proceeding F, **140**(2), 107-113 (1993).
[16] W.R. Gilks, S. Richardson and D.J. Spiegelhalter, Markov chain Monte Carlo in practice, (Chapman & Hall, 1996).
[17] G. Kitagawa, Monte Carlo filter and smoother for non-Gaussian nonlinear state space models, Journal of Computational Graphics and Statistics, **5**, 1-25 (1996).
[18] H. Tanizaki, Nonlinear filters: estimation and applications, (Springer, Berlin, 1996).
[19] A. Doucet, N. de Freitas and N. Gordon, Sequential Monte Carlo methods in practice, (Springer, New York, 2001).
[20] B. Ristic, S. Arulampallam and N. Gordon, Beyond the Kalman filter: Particle filters for tracking applications, (Artech House, Boston, 2004).
[21] N. Chopin, Central limit theorem for sequential Monte Carlo methods and its application to Bayesian inference, The Annals of Statistics, **32**(4), 2385-2411 (2004).
[22] C.S. Manohar, D. Roy, Monte Carlo filters for identification of nonlinear systems, Sadhana, **31**(4), 99-427 (2006).
[23] S. Ghosh, C.S. Manohar and D. Roy, Sequential importance sampling filters with a new proposal distribution for parameter identification of structural systems, Proceedings of Royal Society of London A **464**, 25-47 (2008).
[24] R. Sajeeb, C.S. Manohar and D. Roy, Control of nonlinear structural dynamical systems with noise using particle filters, Journal of Sound and Vibration, **306**(25), 111-135 (2007) .
[25] J.H. Park, N.S. Namachchivaya and H.C. Yeong, Particle filters in a multiscale environment:Homogenized hybrid particle filter, Journal of Applied Mechanics, **78**, 061001 (2011).
[26] C. Jackson, M.K. Sen and P.L. Stoffa, An efficient stochastic Bayesian approach to optimal parameter and uncertainty estimation for climate model predictions, Journal of Climate, **306**(25), 2828-2841 (2004).
[27] W.P. Gouveia and J.A. Scales, Resolution of seismic waveform inversion: Bayes versus Ocean, Inverse Problems, **13**, 323-349 (1997).
[28] A. Malinverno, Parsimonious Bayesian Markov chain Monte Carlo inversion in a nonlinear geophysical problem, Geophysical Journal International, **151**, 675-688 (2002) .
[29] J. Wang and N. Zabaras, Hierarchial Bayesian models for inverse problems in heat conduction, Inverse Problems, **21**, 183-206 (2005).

[30] J. Wang and N. Zabaras, Using Bayesian statistics in the estimation of heat source in radiation, International Journal of Heat and Mass Transfer, **48**, 15-29 (2005) .
[31] J. Ching, J.L. Beck and K.A. Porter, Bayesian state and parameter estimation of uncertain dynamical systems, Probabilistic Engineering Mechanics, **21**, 81-96 (2006) .
[32] V. Namdeo and C.S. Manohar, Nonlinear structural dynamical system identification using adaptive particle filters, Journal of Sound and Vibration, **306**, 524-563 (2007) .
[33] B. Radhika and C.S. Manohar, Reliability models for existing structures based on dynamic state estimation and data based asymptotic extreme value analysis, Probabilistic Engineering Mechanics, **25**, 393-405 (2010) .
[34] H.A. Nasrellah and C.S. Manohar, A particle filtering approach for structural system identification in vehicle-structure interaction problems, Journal of Sound and Vibration, **329**(9), 1289-1309 (2010).
[35] H.A. Nasrellah and C.S. Manohar, Particle filters for structural system identification using multiple test and sensor data: a combined computational and experimental study, Structural Control and Health Monitoring, **18**, 99-120 (2011).
[36] H.A. Nasrellah and C.S. Manohar, Finite element method based Monte Carlo filters for structural system identification, Probabilistic Engineering Mechanics, **26**, 294-307 (2011).
[37] R. Rangaraj, A. Banerjee and S. Gupta, A particle filter based methodology for identifying fatigue cracks from vibration measurements, Journal of Vibrations and Acoustics, ASME, under review (2012) .
[38] A.I. Khuri and J.A. Cornell, Response surfaces: design and analysis, (Marcel and Dekker, New York, 1997).
[39] S. Gupta and C.S. Manohar, An improved response surface method for the determination of failure probability and importance measures, Structural Safety, **26**, 123-139 (2004) .
[40] N. Wiener, The homogeneous chaos, American Journal of Mathematics, **60**, 897-936 (1938) .
[41] D. Xiu and G.E. Karniadakis, The Weiner-Askey polynomial chaos for stochastic differential equations, SIAM Journal on Scientific Computing, **24**, 619-644 (2002).
[42] R. Ghanem, P.D. Spanos, Stochastic finite element: a spectral approach, Springer-Verlag, Berlin (1991).
[43] D. Xiu, D. Lucor, C.H. Su and G. Karniadakis, Stochastic modeling of flow-structure interaction using generalized polynomial chaos, Journal of Fluids Engineering, ASME, **124**, 51-59 (2002) .
[44] J.A.S. Witteven, S. Sarkar and H. Bijl, Modeling physical uncertainties in dynamic stall induced fluid-structure interaction of turbine blades using arbitrary polynomial chaos, Computers and Structures, **85**, 866-878 (2007) .
[45] A. Desai and S. Sarkar, Analysis of a nonlinear aeroelastic system with parametric uncertainties using polynomial chaos expansion, Mathematical Problems in Engineering, doi:10.1155/2010/379472 (2010).
[46] B.H.K. Lee, L. Jiang and Y.S. Wong, Flutter of an airfoil with a cubic nonlinear restoring force, AIAA 98-1725, 237-257 (1998).
[47] Y.C. Fung, An Introduction to the Theory of Aeroelasticity, (JohnWiley and Sons, New York, 1955).